DOI: https://doi.org/10.68732/7405c5ffd9a8e32a

ISBN: 978-9989-2053-6-1

Physical and analytical modelling of sliding-toppling combined slope failures

S. Yuan, P. Carracelas-Lamela, I. Pérez-Rey & L. R. Alejano
CINTECX, Universidade de Vigo, Grupo GESSMin, 36310, Vigo, Spain
iperez@uvigo.gal
0000-0003-0883-7211

Abstract

Simple failure mechanisms including planar, wedge, toppling and circular failure are typically analysed when studying rock slope stability. However, combined failure mechanisms sometimes take place making rock slopes unstable, so it is convenient to consider their possible occurrence. Despite this, research on combined mechanisms remains limited. Among potential combined failure mechanisms in rock masses reported in the literature, the coupling of sliding in the upper part of the slope and toppling in the front is a possible one. This mechanism has also been observed in masonry retaining walls, where the sliding failure of the backfill induces toppling of the drystone blocks. The main objective of this work is to investigate the stability and failure mechanisms of three different configurations representative of such structures, through an experimental program based on tilt-tests on physical models. The critical tilting angles obtained from the experiments are compared against analytical limit equilibrium estimates, showing good agreement. The slight differences in results observed stem from imperfect granite block cutting, limitations of the testing apparatus and inaccuracies derived from simplifying assumptions. Finally, tentative numerical models are presented, and their results show good agreement with the experimental and analytical ones. While each method has inherent strengths and limitations, their cross-validation offers a more robust analysis of failure mechanisms observed in retaining walls and rock slopes affected by combined failure mechanisms.

Keywords

Rock slope stability, Combined failure mechanisms, Retaining wall, Sliding-toppling instability.

1 Introduction

When assessing rock-slope stability, traditional analyses typically consider four simple failure mechanisms: planar, wedge, circular, and toppling failure (Goodman and Bray 1976). These mechanisms have been widely and successfully applied in slope engineering with excellent results. However, real-world failure cases often involve not a single classic mechanism, but rather the combinations of two or more, where the mechanisms are coupled and interact with each other, resulting in a complex overall behaviour. Although combined failure mechanisms have been identified and studied, research in this area remains limited, and further investigation is deemed to be interesting.

Among potential combined forms, the coupling of sliding (planar or circular) and toppling has been reported in the literature (Alejano et al. 2010; Mohtarami et al. 2014;Wei et al. 2024; Mao et al. 2025).

Fig. 1illustrates various types of mechanisms combining sliding and toppling. In Fig. 1a, b, sliding-toppling cases are depicted, where planar or circular sliding in the upper part drives toppling in the lower part, typically facilitated by a steep joint set dipping against the slope that favours toppling toward the excavation. In Fig. 1c, d, toppling-sliding cases are shown, where toppling occurs in the upper parts of the slope, forcing the lower parts to slide. These mechanisms were proposed as secondary toppling by Goodman and Bray (1976) and Wyllie and Mah (2004) representing instability phenomena triggered by the weakening of the slope toe.

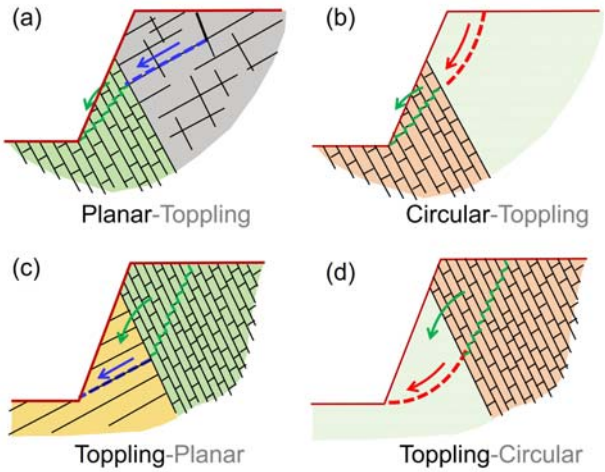


Fig. 1 Schematics of combined failure mechanisms of slope instability: sliding-toppling (planar-toppling (a), and circular-toppling (b)), and toppling-sliding (toppling-planar (c), and toppling-circular (d)).

Simple theoretical methods for computing combined mechanisms are based on limit equilibrium theory, with force transfer between the toppling and sliding parts. The stabilizing force of the upper part of the slope is computed and applied as a load to the lower part, allowing separate stability calculations via traditional methods and overall evaluation based on the stability of the lower part of the slope. For example, Alejano et al. (2010) used this for toppling-sliding. For a sliding-toppling case, applying soil active pressure to the uppermost rock block and analysing toppling is a simple and effective way to assess the mechanism (Mohtarami et al. 2014; Sarfaraz 2020). Physical and numerical methods may validate, supplement, and extend analytical approaches, offering new insights to the study. The sliding-toppling mechanisms herein studied refer to natural rock slopes and engineered structures like dry masonry retaining walls with backfill, where geometry and pressure triggered instability (Alejano et al. 2012; Ding et al. 2025). In these cases, upper backfill slides (following planar or circular surfaces), driving wall toppling and forming a combined failure.

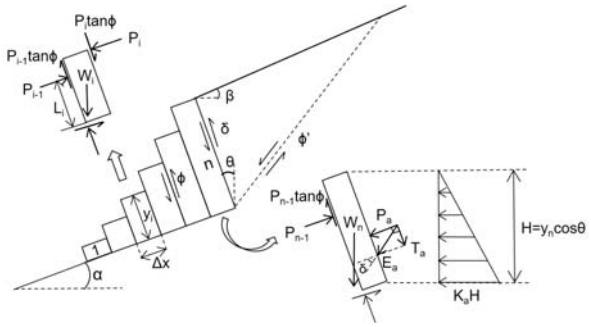


Fig. 2 Schematics and parameters involved in an analytical model of a sliding-toppling combined failure mechanism.

This research seeks to improve safety and economy in wall design and to advance understanding of rock slope stability. This paper proposes a novel analytical model for sliding–toppling failure by integrating classic block toppling theory with Coulomb's earth pressure formulations. Unlike previous studies, this approach captures critical frictional behaviour while significantly simplifying calculations, offering a more practical and efficient framework for engineering applications. Three sets of sliding–toppling lab-scale physical models representing dry masonry retaining walls with granular backfill are designed, prepared and analysed using analytical, physical, and numerical approaches.

2 Theoretical background

Fig. 2 illustrates the elements of the sliding–toppling combined failure mechanism, encompassing a series of blocks and the sliding soil mass behind them. Block toppling is assessed by means of Goodman and Bray (1976) approach. The n^{th} block, with the backfill soil, forms a retaining wall system, and the pressure exerted by the soil is computed according to Coulomb'searth pressure theory.

2.1 Toppling stability

This study adopts the block toppling model proposed by Goodman and Bray (1976), which idealizes the rock mass as a system of 2D rigid, rectangular columns resting on an inclined base. Each block is assumed to rotate about its bottom edge, and toppling stability is evaluated through sequential moment equilibrium analyses of individual blocks. The stabilizing force required for the uppermost block (i = n), is defined by Eq. 1, where active earth pressure is applied as a load on the block.

$$P_{i-1} = \frac{1}{L_i}\left(W_i \sin\alpha \frac{y_i}{2} + E_a \cos\delta \frac{y_i}{3} - W_i \cos\alpha \frac{\Delta x}{2} - E_a \sin\delta\, \Delta x\right) \quad (1)$$

Where P_{i-1} force required to stabilize block i(kN)
L_i lever arm of force P_{i-1}(m)
W_i weight of block i(kN)
α angle of the base plane (tilt or inclination angle)(°)
y_i height of block i(m)
E_a Coulomb active earth pressure(kN)
δ friction angle between the wall and the backfill(°)
Δx width of the block(m)
ϕ friction angle between blocks(°)

The stabilizing forces for the remaining blocks, P_{i-1}, are given by Eq. 2.

$$P_{i-1} = \frac{1}{L_i}\left(W_i \sin\alpha \cdot \frac{y_i}{2} + P_i y_i - W_i \cos\alpha \frac{\Delta x}{2} - P_i \tan\phi\, \Delta x\right) \quad (2)$$

For stability assessment, if the first block (i=1) has P_0>0, indicating instability, the system friction angle is increased until P_0 approaches zero; if P_0<0, it is decreased until the limit state is reached. The friction angle at this condition is defined as the required friction angle, while the material-provided value is the available friction angle. The factor of safety (FoS) is defined by Eq. 3.

$$FoS = \frac{tan(\phi_{available})}{tan(\phi_{required})} \quad (3)$$

2.2 Active earth pressure calculation

For simplified analysis, planar sliding is assumed, and Coulomb's active earth pressure theory is adopted to evaluate the driving force, assuming a cohesionless backfill (c = 0). The active earth pressure acting on the uppermost rock column is given by:

$$E_a = \frac{1}{2} K_a \gamma H^2 \quad (4)$$

Where K_a Coulomb active earth pressure coefficient
γ unit weight of the backfill(kN/m^3)
H vertical height of the wall(m)

The point of application of the earth pressure is at 1/3 of the wall height from the bottom of the wall. Its direction forms an angle δ with the direction perpendicular to the wall. The active earth pressure coefficient K_a is calculated using Coulomb's theory. Its expression is:

$$K_a = \frac{\cos^2(\phi' - \theta)}{\cos\theta + \sin\phi' \sqrt{\frac{(1+\tan\delta/\tan\phi')(1-\tan\beta/\tan\phi')}{(1-\tan\theta\tan\delta)(1+\tan\theta\tan\beta)}}} \quad (5)$$

Where ϕ' friction angle of the backfill(°)
θ inclination angle of the wall(°)
β slope angle of the backfill(°)

2.3 Tilt tests and physical modelling

In analytical methods, the critical inclination angle can be obtained by varying the value of α in the governing equations. In physical modelling, the tilt test provides a simple and effective laboratory approach to determine α and has been widely used to investigate block toppling and wall overturning (Pérez-Rey et al. 2021; Alejano et al. 2015; Gui et al. 2023;Ding et al. 2025), as well as sliding–toppling and toppling–sliding combined failure mechanisms (Amini et al. 2017, 2018). In a tilt test, the inclination of the bearing surface is gradually increased, thereby amplifying the gravity component in the toppling direction until the destabilising moment exceeds the stabilising moment. The corresponding critical inclination angle represents the limit state of system stability and directly reflects the influence of block geometry, centroid position, and interface friction. This method also provides a physical basis for analytical and numerical analyses.

3 Experimental program

3.1 Analytical models

Three analytical models with different number of block rows (n), namely Model I (n=1), Model II (n=2), and Model III (n=3), are developed to investigate the sliding-toppling combined mechanism. When the model is inclined at an angle α, the backfill slope becomes $\beta = \alpha$, and the rock column inclination is $\theta = \alpha$. The process begins by calculating the active earth pressure under inclination α (using the method in Section 2.2) to determine the required force P_{n-1} for the uppermost block (Eq. 1). Eq. 2 is then applied sequentially to compute the required stabilizing forces P_{i-1} for the remaining blocks. By iteratively adjusting α to make P_0= 0, the critical inclination angle is obtained, where the factor of safety equals 1. For non-critical α values, the friction angle is adjusted to set P_0 = 0, and the factor of safety is calculated using Eq. 3.

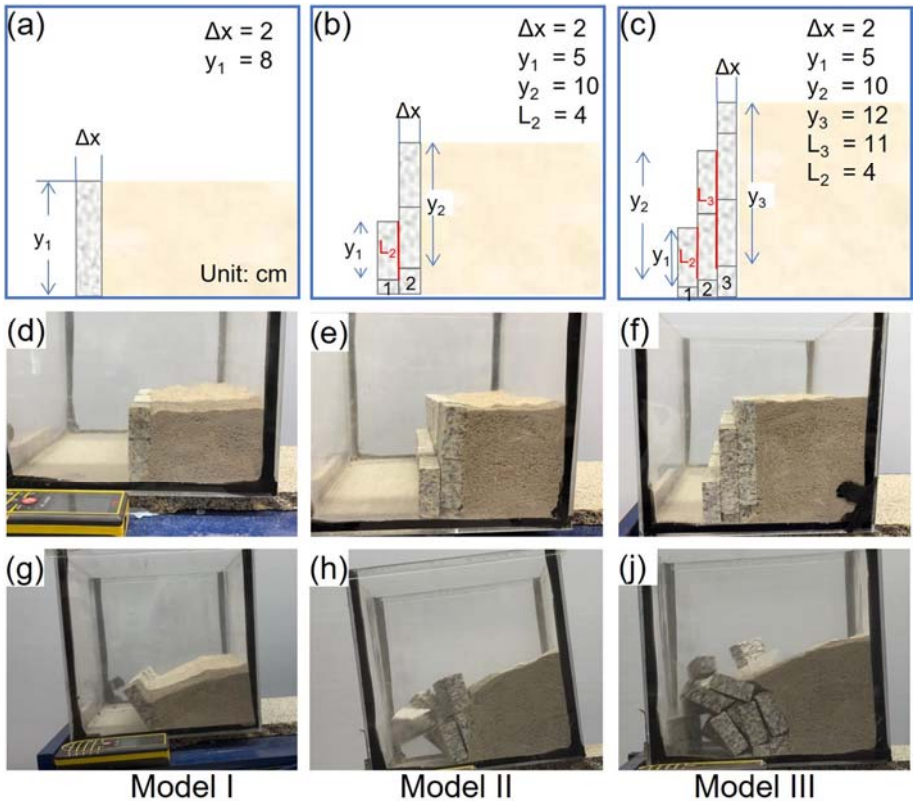


Fig. 3 Experimental results of the analytical models. The schematics in the top row (a-c) depict the analytical models and dimensions, the middle row (d-f) shows the horizontal state at the beginning of the experiment, and the bottom row (g-i) shows the failure moment when reaching the critical inclination angle.

3.2 Physical-modelling experiments and results

Corresponding physical models were constructed based on the analytical setups. The models consist of saw-cut granite blocks with sand backfill and are housed in transparent acrylic boxes mounted on a motor-driven tilting platform rotating at a constant rate of 10°/min. The critical inclination angle at failure onset was recorded, and each experiment was repeated five times. The basic properties of the

granite and sand are listed in Table 1, and the geometric dimensions of the models are shown in the upper part of Fig. 3.

By substituting these geometric parameters along with those from Table 1into the analytical formulas described in Section 2, the critical inclination angles for the models can be determined. Photographs of the experimental process for the physical models are shown in the middle row (horizontal) and the bottom row (tilting failure) of Fig. 3.Each model underwent five repeated tests to obtain the critical inclination angles. The comparison between the analytical, physical and the later obtained numerical values of the critical inclination angle is summarized in Table 2.

Table 1. Parameters of material unit weight and friction angle.

Parameter(unit)	Value
Granite unit weight (kN/m³)	25.31
Sand unit weight γ (kN/m³)	16.02
Sand friction angle ϕ' (°)	30
Sand-granite friction angle δ (°)	28.70
Granite-granite friction angle ϕ (°)	27.72

Table 2. Analytical, experimental, and numerical critical inclination angles for the three models (mean values in parentheses).

Method	Model I (°)	Model II (°)	Model III (°)
Analytical	4.46	3.87	2.95
Physical	3.6–4.6 (4.12)	3.1–4.7 (3.76)	1.9–3.5 (2.36)
Numerical	4.5	3.9	3.0

The results in Table 2 show that the critical inclination angles calculated using the analytical method fall within the range of the physical experimentally measured values. This indicates that the analytical method can effectively capture the sliding-toppling failure mechanism. However, the average experimental values are slightly (0.1 to 0.6º) lower than the analytical predictions. This discrepancy is attributed to block cutting imperfections, such as corner rounding, which affects toppling mechanisms (Alejano et al. 2015).

4 Numerical analyses

Numerical analyses with UDEC 7.0 (Itasca, 2024) were conducted for comparison with results from the other approaches. The wall models were discretized according to their geometry (Fig. 3). In the numerical models, granite is treated as rigid blocks and backfill is a Mohr-Coulomb material with null cohesion, elastic modulus of 10 MPa, and Poisson's ratio of 0.3. The contacts between walls and between walls and backfill are assigned the Coulomb slip criterion, with no cohesion, normal stiffness of 5 GPa/m, and shear stiffness of 1 GPa/m. The friction angles and unit weights of the involved materials are consistent with those in Table 1.

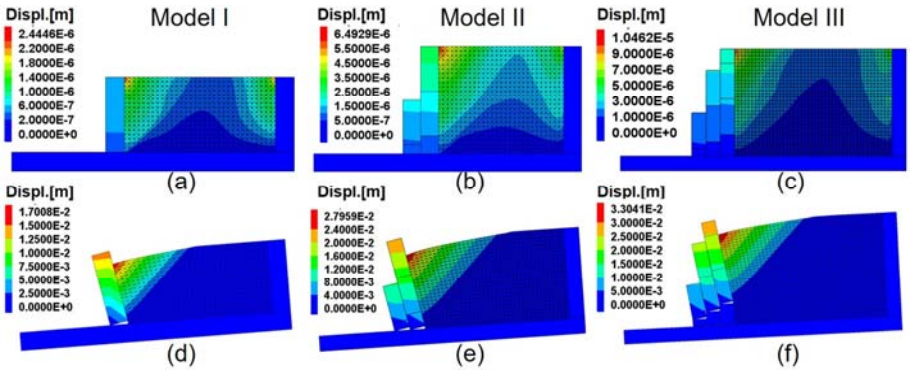


Fig. 4 Total displacement distributions of the three models analysed by UDEC. The upper row (a-c) corresponds to the horizontal condition, and the lower row (d-f) corresponds to the critical inclination angle condition.

The displacement diagrams of the models in the horizontal position and at the critical inclination angle (Table 2) are shown in Fig. 4. From these diagrams, the phenomena of wall toppling and planar sliding of the backfill can be observed, which align with the assumptions and experimentalobservations. Additionally, they capture aspects overlooked by the analytical model. The analytical model simplifies

material deformation and the distribution of contact forces between material interfaces. Therefore, deviations may occur in the safety assessment and critical inclination angle calculations.

5 Concluding remarks

This study investigates the sliding–toppling combined failure mechanism using analytical, physical, and numerical methods. An analytical model evaluates the stability of planar-toppling-prone structures, like dry masonry retaining walls with backfill, by varying the inclination angle. Physical tests successfully reproduce this failure, yielding critical angles that match analytical calculations and are further corroborated by numerical simulations

Discrepancies indicate that physical model failures occur at slightly lower inclination angles than analytical predictions. This behaviour is primarily attributed to geometric imperfections of granite blocks, such as rounded edges, which modify moment arms and centres of gravity. Furthermore, experimental boundary conditions and numerical parameters, particularly contact and elastic properties, significantly influence the results. Due to scaling effects, small laboratory models fail to capture the roughness, joint strength, and corner rounding inherent in large field structures. The impact of these size-dependent features will be addressed in future work.

By cross-validating analytical, physical, and numerical methods, this study provides a comprehensive understanding of the sliding–toppling combined failure mechanism and contributes to improved insight into the stability behaviour of rock slopes.

References

Alejano LR, Carranza-Torres C, Giani GP, Arzúa J (2015) Study of the stability against toppling of rock blocks with rounded edges based on analytical and experimental approaches. Eng Geol 195:172–184. https://doi.org/10.1016/j.enggeo.2015.05.030

Alejano LR, Gómez-Márquez I, Martínez-Alegría R (2010) Analysis of a complex toppling-circular slope failure. Eng Geol 114:93–104. https://doi.org/https://doi.org/10.1016/j.enggeo.2010.03.005

Alejano LR, Veiga M, Taboada J, Díez-Farto M (2012) Stability of granite drystone masonry retaining walls: I. Analytical design. Geotechnique 62:1013–1025. https://doi.org/10.1680/geot.10.P.112

Amini M, Ardestani A, Khosravi MH (2017) Stability analysis of slide-toe-toppling failure. Eng Geol 228:82–96. https://doi.org/https://doi.org/10.1016/j.enggeo.2017.07.008

Amini M, Sarfaraz H, Esmaeili K (2018) Stability analysis of slopes with a potential of slide-head-toppling failure. International Journal of Rock Mechanics and Mining Sciences 112:108–121. https://doi.org/https://doi.org/10.1016/j.ijrmms.2018.09.008

Ding B, Pérez-Rey I, González-Fernández MA, et al (2025) Optimizing shape design in drystone retaining walls: A multi-scope approach focusing on failure mechanisms. Constr Build Mater 489:142116. https://doi.org/https://doi.org/10.1016/j.conbuildmat.2025.142116

Goodman RE, Bray JW (1976) toppling of rock slopes. In: Proceedings of the Specialty Conference on Rock Engineering for Foundation and Slopes ASCE Boulder. Colorado

Gui JY, González-Fernández MA, Estévez-Ventosa X, et al (2023) Toppling susceptibility of a single rock block resting on a regularly rough base. Eng Geol 83:153. https://doi.org/10.1016/j.enggeo.2022.106982

Itasca Consulting Group (2024) UDEC. Universal distinct element code. Itasca, Minneapolis, USA.

Mao Y, Azarafza M, Bonab MH, et al (2025) Innovative stability analysis of complex secondary toppling failures in rock slopes using the block theory. Landslides 22:2037-2054. https://doi.org/10.1007/s10346-025-02464-4

Mohtarami E, Jafari A, Amini M (2014) Stability analysis of slopes against combined circular-toppling failure. International Journal of Rock Mechanics and Mining Sciences 67:43–56. https://doi.org/10.1016/j.ijrmms.2013.12.020

Pérez-Rey I, Muñiz-Menéndez M, González J, et al (2021) Laboratory physical modelling of block toppling instability by means of tilt tests. Eng Geol 282:105994. https://doi.org/10.1016/j.enggeo.2021.105994

Sarfaraz H (2020) A simple theoretical approach for analysis of slide-toe-toppling failure. J Cent South Univ 27:2745–2753. https://doi.org/10.1007/s11771-020-4495-7

Wei T, Chen GQ, Zhu Z, et al (2024) Slope instability mechanism with differential rock mass structure along a fault: a mine landslide from Southwest China. Geomechanics and Geophysics for Geo-Energy and Geo-Resources 10:76. https://doi.org/10.1007/s40948-024-00795-5

Wyllie DC, Mah CW (2004) Rock slope engineering: fourth edition. CRC Press, London